PAPER

The role of solvation in proton transfer reactions: implications for predicting salt/co-crystal formation using the ΔpK_a rule†

Aurora J. Cruz-Cabeza, [iD] *[ab] Matteo Lusi, [iD] [c] Helen P. Wheatcroft[b] and Andrew D. Bond [iD] [d]

The ΔpK_a rule is commonly applied by chemists and crystal engineers as a guideline for the rational design of molecular salts and co-crystals. For multi-component crystals containing acid and base constituents, empirical evidence has shown that $\Delta pK_a > 4$ almost always leads to salts, $\Delta pK_a < -1$ almost always leads to co-crystals and ΔpK_a between -1 and 4 can be either. This paper reviews the theoretical background of the ΔpK_a rule and highlights the crucial role of solvation in determining the outcome of the potential proton transfer from acid to base. New data on the frequency of the occurrence of co-crystals and salts in multi-component crystal structures containing acid and base constituents show that the relationship between ΔpK_a and the frequency of salt/co-crystal formation is influenced by the composition of the crystal. For unsolvated co-crystals/salts, containing only the principal acid and base components, the point of 50% probability for salt/co-crystal formation occurs at $\Delta pK_a \approx 1.4$, while for hydrates of co-crystals and salts, this point is shifted to $\Delta pK_a \approx -0.5$. For acid–base crystals with the possibility for two proton transfers, the overall frequency of occurrence of any salt (monovalent or divalent) *versus* a co-crystal is comparable to that of the whole data set, but the point of 50% probability for observing a monovalent salt *vs.* a divalent salt lies at $\Delta pK_{a,II} \approx -4.5$. Hence, where two proton transfers are possible, the balance is between co-crystals and divalent salts, with monovalent salts being far less common. Finally, the overall role played by the "crystal" solvation is illustrated by the fact that acid–base complexes in the intermediate region of ΔpK_a tip towards salt formation if ancillary hydrogen bonds can exist. Thus, the solvation strength of the lattice plays a key role in the stabilisation of the ions.

[a]*Department of Chemical Engineering, School of Engineering, University of Manchester, UK. E-mail: aurora.cruzcabeza@manchester.ac.uk*

[b]*Chemical Development, Pharmaceutical Technology & Development, AstraZeneca, Macclesfield, UK*

[c]*Department of Chemical Sciences, Bernal Institute, University of Limerick, Limerick, Ireland*

[d]*Yusuf Hamied Department of Chemistry, University of Cambridge, Cambridge, UK*

† Electronic supplementary information (ESI) available. See DOI: 10.1039/d1fd00081k

Introduction

Proton transfer reactions between an acid and a base are responsible for many natural phenomena, from the existence of salts to the zwitterionic nature of common amino acids in environments amenable to life, or the interactions between proteins and substrates. From a chemical point of view, acid–base equilibria can easily be studied. In particular, the activity (or concentration) of ionised species can be measured in solution and acid dissociation constants (K_a) calculated and reported, typically in the form of pK_a values. Moreover, robust computational models have been developed to predict aqueous pK_a values from the molecular structure.[1–3]

Proton transfer is also common in the solid state, as demonstrated by the large number of molecular salts[4] and zwitterionic crystal structures reported in the Cambridge Structural Database (CSD).[5] In molecular crystals, proton transfer reactions generally lie fully to one side of the chemical equation, yielding either a co-crystal where no proton transfer occurs or a salt where a proton is transferred from an acid to a base. Exceptions include dynamic systems, such as solid-state proton conductors,[6] or cases in which protons appear to be located part way between the acid and the base.[7] The characterisation of such systems can be complicated by the inherent difficulties associated with locating H atoms using X-ray diffraction data, and in some cases the extent of proton transfer may be temperature dependent.[8,9] Because of this, complementary characterisation techniques, such as XPS,[10–12] solid-state NMR[13] or neutron diffraction[14,15] (amongst others[16]), often need to be used to locate precisely the position of the acid H atoms. There are also cases where both ionised and non-ionised species of an acid or base are present in the same crystal.[17]

The ionisation of active pharmaceutical ingredients (APIs) into salts plays a crucial role in the formulation of medicines.[4,18] Salts are often more soluble than their corresponding non-ionised forms, thereby affording drugs with improved pharmacokinetics.[19] In recent years, co-crystals have been shown to be a viable alternative to salts since they can also improve the solubility of APIs[20] whilst offering other advantages, such as being less prone to hydration.[21] Co-crystals are often designed using crystal engineering concepts,[22–25] whereby suitable co-crystal formers are selected based on their potential to form strong molecule-to-molecule interactions (synthons), typically based on hydrogen bonds.[26–28] Very often, the targeted interactions involve an acid and a base. Indeed, hydrogen bonds are particularly strong, and therefore most attractive for crystal engineering strategies, for acid–base pairs with $\Delta pK_a \approx 0$, where $\Delta pK_a = pK_a(\text{protonated base}) - pK_a(\text{acid})$.[29,30] However, such strategies may be compromised by proton transfer in the solid state, thereby yielding a salt rather than the intended co-crystal product.

As a rule of thumb, salt formation in a molecular crystal is typically considered to be likely if the ΔpK_a for the constituent acid and base is larger than 3. In 2005, Bhogala *et al.*[31] noted that negative values of ΔpK_a always lead to the formation of co-crystals. This so-called "ΔpK_a rule" has been commonly used for the rational design of salts and co-crystals, supported by the free availability of experimental and calculated pK_a data. In 2012, Cruz-Cabeza revised the rule on the basis of a survey of *ca.* 6500 crystal structures and pK_a values calculated for the molecular components.[32] It was found that $\Delta pK_a > 4$ almost always leads to salts, $\Delta pK_a < -1$

almost always leads to co-crystals and ΔpK_a between −1 and 4 can be either. The intermediate region of ΔpK_a accommodates what Childs has referred to as the salt/co-crystal continuum.[33]

Given the enduring popularity of the ΔpK_a rule amongst chemists and crystal engineers,[34–36] this paper sets out to review the theoretical basis of the rule, highlighting (in particular) the role of solvation for determining the outcome of proton transfer reactions in the solid state. When applying the ΔpK_a rule to predict salt/co-crystal formation, a key question is how the crystal lattice influences proton transfer, particularly in the intermediate region close to $\Delta pK_a \approx 0$. Some new data extracted from an extensive set of crystal structures demonstrates how the ΔpK_a rule might be fine-tuned for specific classes of crystals, such as crystalline hydrates. Analysis of those structures also reveals the important role played by ancillary hydrogen-bonds in stabilising ionisation in the solid-state.

Methods

pK_a and ΔpK_a calculations

pK_a values were calculated using ChemAxon's Marvin software suite (version 21.13),[37] either through the visualiser or via the command line executable for the bulk processing of many compounds. The calculator returns pK_a values for both acids and protonated bases (depicted in the visualiser in red and blue, respectively). The ΔpK_a for an acid–base pair was then calculated by subtracting the pK_a values of the strongest acid and strongest base, where $\Delta pK_a = pK_a(BH^+) - pK_a(A)$. For systems where a second proton transfer is possible, a second value of ΔpK_a, denoted $\Delta pK_{a,II}$, was also calculated. For this calculation, the stoichiometry of the system was accounted for when considering the second-strongest acid and base. For example, the first ΔpK_a uses the lowest $pK_a(A)$ and the highest $pK_a(BH^+)$ in the crystal structure (i.e. the strongest acid and strongest base) and the second $\Delta pK_{a,II}$ would use the second lowest $pK_a(A)$ and the second highest $pK_a(BH^+)$. Depending on the crystal composition and stoichiometry, the second base could be the same as the first for a $H_2A : B$ system with a 1 : 2 stoichiometry (resulting in $\{A^{2-}\}\{BH^+\}_2$) or it could be the second strongest basic functional group in the base for a system with a 1 : 1 stoichiometry (resulting in $\{A^{2-}\}\{BH_2^{2+}\}$). The ΔpK_a values were obtained from the calculated pK_a values using a simple Python script. Finally, it was recorded whether the acid–base pair for each ΔpK_a calculation was located within the same molecule or in different molecules. This differentiates ΔpK_a values for intermolecular proton transfer (salt formation) from $\Delta pK_{a,self}$ values for intramolecular proton transfer (zwitterion formation).

Energy calculations

Energy calculations were performed with Gaussian 16 (ref. 38) using the B97d level of theory and the 6-31+G(d,p) basis sets.[39] For the calculation of $\Delta E_{ion\text{-}gas}^{\circ HA \cdot B}$, ions, as well as neutral species, were optimised separately and the term $\Delta E_{ion\text{-}gas}^{\circ HA \cdot B}$ was calculated as the difference between the electronic energy of the ions minus the electronic energy of the neutral species. Implicit solvation models (SMD)[40] for toluene, 2-heptanone and water were also used for some calculations. For the calculation of the potential energy for proton transfer in acid–base pairs, molecular models were generated manually using Avogadro[41,42] and initially optimised using

the MMFF94s forcefield.[43] The resulting model for the acid–base dimer was then optimised in the gas phase using Gaussian. In all cases, the acid and base were oriented to form an A–H⋯B hydrogen bond. The resulting geometry (containing neutral species in all cases) was then used to run constrained optimisations in various media (gas phase, toluene, 2-heptanone and water). Here, the distance between the acid proton and the acceptor atom of the base was constrained progressively in the range of −0.8 to +2.4 Å in steps of 0.1 Å. Energies are reported relative to the best non-ionised gas-phase geometry in each case.

Datasets of crystal structures

Crystal structure datasets were built following the steps depicted in Fig. 1. The CSD version 5.42 (ref. 44) was first filtered for structures containing any combination of the atom types H, C, O, S and halogens, and with determined 3D coordinates. Only organic structures were thus retrieved. This yielded over 215k structures of single-component crystals and over 61k structures of multi-component crystals.

The CSD Python API interface was then used to generate SMILES strings for all components in the crystal structures, and the stoichiometry and nature of the components were established. Components with a positive charge were designated as cations, those with a negative charge as anions, and those with separation of charges within the same compound as zwitterions (which could also be anions or cations depending on the overall charge). Cations and zwitterions were further classified as quaternary (Q4) if the positive charge was not due to proton transfer (e.g. N^+ bonded to four other C atoms). The SMILES of neutral components were checked and flagged as water, solvent (if within the 18 most common solvent types in the CSD) or main molecular component. Most of the total 276k retrieved crystal structures passed successfully through the pK_a calculator, but some failed due to errors, disorder or uncommon SMILES strings. The final dataset-1 contained nearly 259k crystal structures with calculated pK_a values.
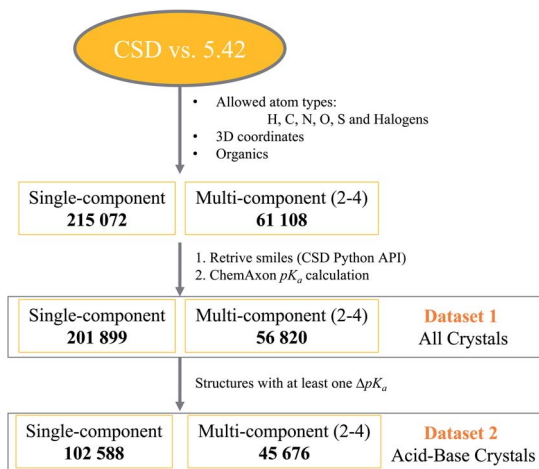

Fig. 1 Process for the retrieval of dataset-1 and dataset-2.

Dataset-1 was then filtered for structures containing at least one acid–base pair, and thus one ΔpK_a value, resulting in dataset-2, containing over 148k crystal structures. A Python script was written to analyse all data. The number of protons transferred in each crystal structure was recorded, as well as the location of the strongest acid and base. If the strongest acid and base were contained within the same molecule, ΔpK_a was classified as $\Delta pK_{a,self}$ and these data were used for the analysis of trends in zwitterions and neutral compounds. If the strongest acid and base were contained within different molecules in the crystal, this was classified as a standard ΔpK_a. Second strongest acids and bases were also considered and $\Delta pK_{a,II}$ was recorded for relevant structures.

Full interaction maps

Full interaction maps (FIMs)[45] were calculated for pairs of acids and bases using a water oxygen as a probe and displaying only the third contour with the standard setting of 6.0 (higher localised special probability). This was done using Mercury version 2021.2.0.[46]

### Hydrogen bond analysis in salts and co-crystals with $\Delta pK_a \approx 0$

In total, 818 structures of co-crystals and monovalent salts with $\Delta pK_a \approx 0$ (within an absolute tolerance of 1 unit, ΔpK_a values between -0.5 and 0.5) were identified in dataset-2. These crystal structures were loaded into Conquest and the hydrogen-bonding environments of the acid–base pairs were analysed. First, the set was filtered to structures containing an acid–base contact involving a carboxylic acid/carboxylate. This resulted in a subset of 531 structures. The ancillary hydrogen bonds (HBs) around the carboxylic acid/carboxylate were then analysed further and structures grouped into three subsets: structures with 0, 1 or 2 ancillary HBs. For this purpose, Conquest queries were built for the different HB environments, with HBs identified as follows:

- The HB donor is either an N or an O atom (no C atoms).
- The HB acceptor is either O or the O^- in the carboxylic acid or carboxylate, respectively.
- The distance between the non-H atoms involved in the HB is less than the sum of their van der Waals radii.
- The angle of the HB (N/O–H···O/O$^-$) is between 120 and 180°.
- Both intramolecular and intermolecular HBs were recorded.

Theoretical background

Gibbs free energy and ΔpK_a

For the dissociation of a monoprotic acid (HA) in water, the equilibrium is quantified by the acid dissociation constant, K_a^{HA}:

$$HA(aq) + H_2O(l) \xrightleftharpoons{K_a^{HA}} A^-(aq) + H_3O^+(aq)$$
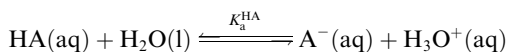
For a monoprotic base (B) accepting a proton in water, it is convenient also to quantify the equilibrium using the acid dissociation constant of the protonated base, $K_a^{BH^+}$:

$$BH^+(aq) + H_2O(l) \underset{\phantom{K_a^{BH^+}}}{\overset{K_a^{BH^+}}{\rightleftharpoons}} B(aq) + H_3O^+(aq)$$
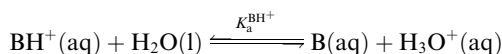
Since an equilibrium between HA and B in aqueous solution is a combination of the acid and base equilibria, the equilibrium constant can be expressed as a quotient of the individual acid dissociation constants:

$$HA(aq) + B(aq) \rightleftharpoons A^-(aq) + BH^+(aq)$$
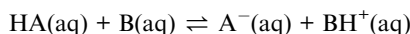
$$K_{\text{ion-water}}^{\text{HA} \cdot \text{B}} = \frac{K_a^{HA}}{K_a^{BH^+}}$$

Taking logarithms equates the log of the equilibrium constant for the proton transfer reaction in water to ΔpK_a:

$$\log K_{\text{ion-water}}^{\text{HA} \cdot \text{B}} = \log K_a^{HA} - \log K_a^{BH^+} = pK_a^{BH^+} - pK_a^{HA} = \Delta pK_a$$

Using the thermodynamic relation between the standard Gibbs free energy of a reaction and its equilibrium constant, the standard free energy change for proton transfer between the acid and base in water is related to ΔpK_a as follows:

$$\Delta G_{\text{ion-water}}^{\circ \text{HA} \cdot \text{B}} = -RT \ln K_{\text{ion-water}}^{\text{HA} \cdot \text{B}} = -2.3RT \log K_{\text{ion-water}}^{\text{HA} \cdot \text{B}} = -2.3RT\Delta pK_a$$

At 298 K, $\Delta G_{\text{ion-water}}^{\circ \text{HA} \cdot \text{B}} = -5.71 \, \Delta pK_a$. Thus, positive values of ΔpK_a correspond to negative $\Delta G_{\text{ion-water}}^{\circ \text{HA} \cdot \text{B}}$ and therefore favour proton transfer from acid to base. Negative values of ΔpK_a correspond to positive $\Delta G_{\text{ion-water}}^{\circ \text{HA} \cdot \text{B}}$ and favour non-ionised acid and base. Each additional unit of ΔpK_a changes $\Delta G_{\text{ion-water}}^{\circ \text{HA} \cdot \text{B}}$ by ± 5.71 kJ mol^{-1}. For $\Delta pK_a = 0$, $\Delta G_{\text{ion-water}}^{\circ \text{HA} \cdot \text{B}} = 0$, giving equal quantities of ionised and non-ionised species in water. Most pK_a data refer to an aqueous solution at 298 K. However, the values may change drastically in other solvents and media.[47]

Extension to molecular crystals

The formation of a multi-component molecular crystal comprising an acid and a base may yield either a salt if proton transfer occurs or a co-crystal if there is no proton transfer. A thermochemical cycle summarising the associated free energy changes is shown in Fig. 2. For the co-crystal, the free energy of formation is simply the lattice free energy relative to the non-interacting molecules in the gas phase, $\Delta G_{\text{latt}}^{\circ \text{cocrystal}}$ (assuming no significant conformational change for the molecules upon crystallisation). For the salt, the free energy of formation is the sum of the free energy for proton transfer in the gas phase, $\Delta G_{\text{ion-gas}}^{\circ \text{HA} \cdot \text{B}}$, plus the lattice free energy of the salt relative to the non-interacting ions in the gas phase, $\Delta G_{\text{latt}}^{\circ \text{salt}}$. Hence, the formation of a salt or co-crystal (under thermodynamic control) depends on the balance between the free energy for proton transfer in the gas phase and the difference between the lattice free energies of the salt and co-crystal:
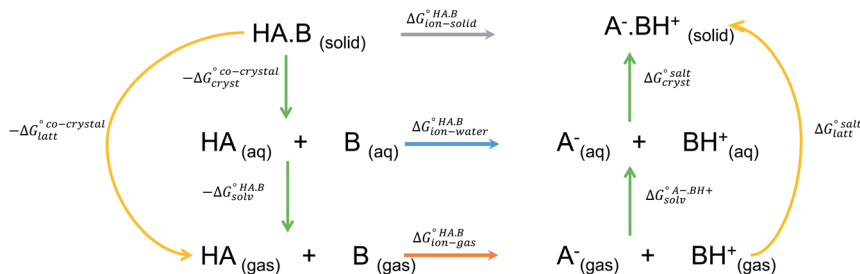
Fig. 2 Thermochemical cycle summarising the free energy changes associated with the formation of a molecular salt or co-crystal.

$$\Delta G_{\text{ion-solid}}^{\circ\,\text{HA}\cdot\text{B}} = \Delta G_{\text{ion-gas}}^{\circ\,\text{HA}\cdot\text{B}} + \left(\Delta G_{\text{latt}}^{\circ\,\text{salt}} - \Delta G_{\text{latt}}^{\circ\,\text{cocrystal}}\right) \tag{1}$$

If $\Delta G_{\text{ion-solid}}^{\circ\,\text{HA}\cdot\text{B}} < 0$, a salt will be favoured over a co-crystal. Conversely, if $\Delta G_{\text{ion-solid}}^{\circ\,\text{HA}\cdot\text{B}} > 0$, a co-crystal will be preferred.

Evaluating $\Delta G_{\text{ion-solid}}^{\circ\,\text{HA}\cdot\text{B}}$: the gas-phase route

Since temperature and entropic effects remain challenging to compute and their relative changes are typically small,[48] the standard free energy differences can be approximated to potential energy changes at 0 K, so:

$$\Delta G_{\text{ion-solid}}^{\circ\,\text{HA}\cdot\text{B}} \approx \Delta E_{\text{ion-solid}}^{\text{HA}\cdot\text{B}} = \Delta E_{\text{ion-gas}}^{\text{HA}\cdot\text{B}} + \left(\Delta E_{\text{latt}}^{\text{salt}} - \Delta E_{\text{latt}}^{\text{cocrystal}}\right) \tag{2}$$

where the first term, $\Delta E_{\text{ion-gas}}^{\text{HA}\cdot\text{B}}$, is the energy for proton transfer in the gas phase, and the second term is the difference in lattice energies between the resulting salt and co-crystal.

Although less commonly reported than pK_a values, proton affinities (PA) in the gas phase can be measured or computed, which enables $\Delta E_{\text{ion-gas}}^{\circ\,\text{HA}\cdot\text{B}}$ to be determined as follows:

$$\text{PA(acid)} = \Delta E^{\circ}\{A^-(g) + H^+(g) \rightarrow HA(g)\}$$

$$\text{PA(base)} = \Delta E^{\circ}\{B(g) + H^+(g) \rightarrow BH^+(g)\}$$

$$\Delta E_{\text{ion-gas}}^{\circ\,\text{HA}\cdot\text{B}} = \text{PA(base)} - \text{PA(acid)}.$$

The second term in eqn (2) is usually highly negative because lattice energies of salts are significantly more negative than those of co-crystals due to the coulombic contributions in the salt, and the first term in eqn (2) is usually highly positive (energy is required for proton transfer). It is the balance between $\Delta E_{\text{ion-gas}}^{\circ\,\text{HA}\cdot\text{B}}$ and $(\Delta E_{\text{latt}}^{\text{salt}} - \Delta E_{\text{latt}}^{\text{co-crystal}})$ that determines whether a co-crystal would form.

In this context, ΔpK_a can be viewed as a proxy estimate for $\Delta E_{\text{ion-gas}}^{\circ\,\text{HA}\cdot\text{B}}$. In general, the strengths of acids and bases in aqueous solution do not necessarily correspond to the proton affinities in the gas phase, but a good linear dependence

between the gas phase and aqueous acidity has been shown for organic acids of the type typically found in molecular crystals.[49] If HA is a strong acid and B is a strong base (leading to a large positive ΔpK_a), $\Delta E_{\text{ion-gas}}^{\circ \text{HA} \cdot \text{B}}$ is likely to be less positive and amply compensated by the lattice energy gain of the salt. If HA and B are a weak acid/base (leading to a negative ΔpK_a), $\Delta E_{\text{ion-gas}}^{\circ \text{HA} \cdot \text{B}}$ will have a larger positive value which could outweigh the energy gain of the salt lattice and therefore favour the co-crystal. For intermediate cases, the balance is delicate.

If a crystal structure (or structures) is known, the difference in lattice energy between the salt and co-crystal can be explicitly calculated for a given system.‡ For example, Mohamed *et al.* have shown the energetic balance between a salt and co-crystal for a series of pyridine/carboxylic acid crystals.[50] In this series, the acid and base interact directly in the crystal structure so the salt/co-crystal balance can be explored by shifting the acid proton across an O–H···N hydrogen bond. In some cases, a single-well potential was found with a clearly favoured position (either co-crystal or salt), but other cases showed a very shallow potential with very little energetic difference between either situation.[50] Similar studies on a series of hydrazone/dicarboxylic acid crystals produced comparable results.[51] Further to this, commonly applied DFT-D methods have been shown to often result in incorrect proton transfer in acid–base cocrystals.[53] Hence, the second term in eqn (2) may need careful consideration on a crystal-by-crystal basis. The biggest limitation here, of course, is the requirement to determine the crystal structure(s) in order to make the calculations. To predict salt/co-crystal formation from the molecular structure alone, the entire process would require crystal structure prediction (CSP) of both the co-crystal and salt systems followed by accurate computation of the lattice energies.[52] Hence, the full evaluation of eqn (2) is generally impractical as a predictive tool.

Evaluating $\Delta G_{\text{ion-solid}}^{\circ \text{HA} \cdot \text{B}}$: the aqueous route

Following the thermochemical cycle in Fig. 2, $\Delta G_{\text{ion-solid}}^{\circ \text{HA} \cdot \text{B}}$ can be calculated from aqueous solution data as follows:

$$\Delta G_{\text{ion-solid}}^{\circ \text{HA} \cdot \text{B}} = \Delta G_{\text{ion-water}}^{\circ \text{HA} \cdot \text{B}} + \left(\Delta G_{\text{cryst}}^{\circ \text{salt}} - \Delta G_{\text{cryst}}^{\circ \text{cocrystal}} \right) \tag{3}$$

where $\Delta G_{\text{cryst}}^{\circ}$ is the standard free energy change upon crystallisation of the salt or co-crystal from the constituent components in aqueous solution. This is the opposite process to that defining the solubility product, and hence $\Delta G_{\text{cryst}}^{\circ} = RT \ln K_{\text{sp}}$, where K_{sp} is the product of the molar concentrations of the molecular constituents in solution. The first term of eqn (3) has been shown earlier to be $-2.3RT\Delta pK_a$, so eqn (3) can be re-written as:

$$\Delta G_{\text{ion-solid}}^{\circ \text{HA} \cdot \text{B}} = -2.3RT \left(\Delta pK_a - \log \left(\frac{K_{\text{sp}}^{\circ \text{salt}}}{K_{\text{sp}}^{\circ \text{cocrystal}}} \right) \right). \tag{4}$$

---

‡ If a classical modelling approach is used, the ionisation term and the lattice energy terms will be computed separately. However, if a quantum modelling approach is used, the lattice energy will be optimised together with the ionisation state. A single optimisation of a crystal structure with DFT-d will result in either a salt or a co-crystal for a single well potential scenario since it will optimise the total energy of the lattice simultaneously.
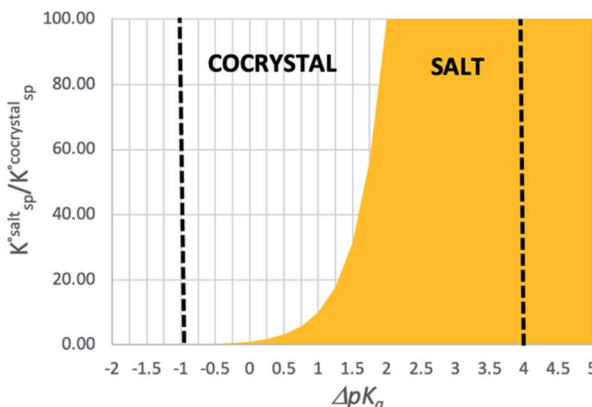
Fig. 3 Diagram showing the regions where salt (yellow) and co-crystal (no fill) are favoured as a function of the ΔpK_a of the acid–base pair and the relative solubility of the salt and the co-crystal.

Using eqn (4), the sign of $\Delta G^{\circ\,\mathrm{HA\cdot B}}_{\mathrm{ion\text{-}solid}}$ and, hence, the relative thermodynamic stability of the salt and co-crystal, can be visualised through a simple diagram (Fig. 3). For each ΔpK_a value, the value of $\log\left(\dfrac{K^{\circ\,\mathrm{salt}}_{\mathrm{sp}}}{K^{\circ\,\mathrm{cocrystal}}_{\mathrm{sp}}}\right)$ at which the free energy of proton transfer is 0 represents the boundary between the co-crystal and salt regions. This diagram illustrates neatly the ΔpK_a rule. Co-crystals dominate when $\Delta pK_a < 0$. When $\Delta pK_a > 4$, salts dominate in most solubility ratio ranges. In the intermediate region of ΔpK_a, the outcome is strongly sensitive to the relative solubility product of the salt *versus* the co-crystal.

While ΔpK_a can easily be measured or calculated, the second term in eqn (4) cannot be quantified unless both a co-crystal and a salt exist for the system, and the solubility products can be measured. This is almost never the case. Hence, eqn (4) is no more practical than eqn (2) as a general predictive tool.

Finally, it should be stressed that the balance between ΔpK_a and the solubility ratio may be complex. For example, in the case where an acid becomes significantly weaker than the expectation in aqueous solution due to a change to a poorly solvating solvent, this may be compensated by a change in the relative solubilities of the co-crystal and the salt. For example, upon changing from water to an organic solvent, the effective ΔpK_a may decrease, but this is likely to be compensated by a decrease in the solubility product of the salt relative to the co-crystal. An example of such behaviour is seen for cediranib maleate.[54] Hence, the applicability of expectations based on an aqueous environment must be carefully considered when transferring to other solvents.

Practical application of the ΔpK_a rule

Although the preceding sections add theoretical context to ΔpK_a as a predictor for salt/co-crystal formation, the practical application of the ΔpK_a rule is effectively based on empirical evidence. While it is unclear when the observation that salts would typically form for acid and bases with $\Delta pK_a > 3$ was made, this knowledge has been used for decades in the pharmaceutical industry. In 2012, Cruz-Cabeza

probed the rule in the CSD and showed that $\Delta pK_a > 4$ almost always leads to salts and $\Delta pK_a < -1$ almost always leads to co-crystals. In the intermediate region, the probability of salt formation was found to follow the empirical trend:

$$P_{obs}(salt, \%) = 17 \, \Delta pK_a + 28$$

In this context, with over 1 million crystal structures now available in the CSD, we set out in this work to probe further the experimental observations of salt and co-crystal formation, in order to shed light on the impact of crystal composition (particularly hydration), the location of the acid and base groups, the local hydrogen-bonding environment and the possibility of further proton transfers on the ΔpK_a rule.

Results

Impact of solvation on the potential energy of acid–base proton transfer

To demonstrate the effect of the acid–base relative strength, as well as solvation, on the ionisation of acid–base pairs, we selected acetic acid (AA) as a model acid together with three bases with increasing base strength: THF, pyridine (PYR) and trimethylamine (TMA). The computed ΔpK_a and $\Delta E_{ion\text{-}gas}^{\circ HA \cdot B}$ values in the gas phase are summarised in Fig. 4. As expected, as ΔpK_a increases, $\Delta E_{ion\text{-}gas}^{\circ HA \cdot B}$ decreases, from 605 kJ mol^{-1} for AA:THF to 330 kJ mol^{-1} for AA:TMA.

To expand on these values, and to illustrate the impact of solvation, the potential energy curve for proton transfer for each acid–base pair was calculated in different solvation environments: (a) gas-phase; (b) toluene; (c) 2-heptanone; (d) water. The solution environments were accounted for implicitly using SMD solvation models. Toluene and 2-heptanone were chosen because their dielectric constants (toluene = 2.3, 2-heptanone = 12) are similar to those anticipated for neutral molecular solids and molecular salts, respectively.[55] Hence, they are intended to give a coarse approximation of the situation that may be found in the crystalline state. They are not necessarily implied to be common laboratory
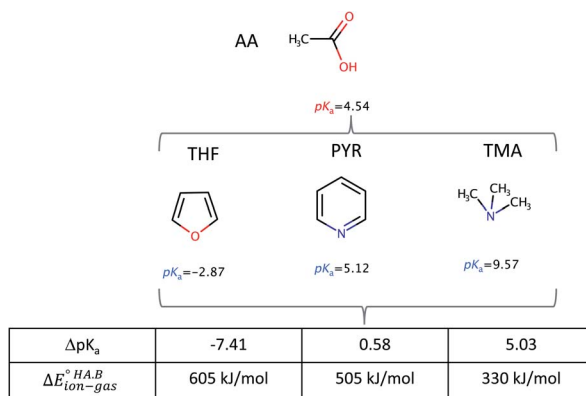

Fig. 4 Calculated ΔpK_a values and gas-phase proton transfer energies for acid–base pairs formed between AA with three bases (THF, PYR, TMA) of increasing strength.

solvents (indeed, 2-heptanone is rare in practice). For the calculations, the AA molecule was located next to the base so that an A–H⋯B hydrogen bond was formed, and the geometry was optimised. The potential energy was then calculated as a function of the position of H^+ within the A–H⋯B hydrogen bond, as outlined in the Methods section. The results are shown in Fig. 5.

For AA:THF ($\Delta pK_a = -7.4$), none of the environments favour proton transfer from acid to base because of the high $\Delta E_{\text{ion-gas}}^{\circ \text{HA} \cdot \text{B}}$ value for this pair. For AA:TMA ($\Delta pK_a = 5.0$), a similar situation is seen in the gas phase, but there is a progressive emergence of an energy minimum for proton transfer as the dielectric constant of the solvent increases. In aqueous solution, the minimum is pronounced and the ionised species are favoured over the neutral species by over 20 kJ mol^{-1}. For AA:PYR ($\Delta pK_a = 0.6$), an intermediate situation is seen, whereby the curve for aqueous solution resembles that for AA:TMA in 2-heptanone. Hence, the balance between $\Delta E_{\text{ion-gas}}^{\circ \text{HA} \cdot \text{B}}$ and the extent to which the ionised species are stabilised by solvation is clearly seen. To extend this picture to the solid state, the key question is how the crystal lattice impacts the outcome. The empirical evidence established for the ΔpK_a rule suggests that the effect of the lattice is never sufficient to influence the outcome for acid–base pairs with $\Delta pK_a < -1$ or $\Delta pK_a > 4$, but that it can have a significant effect in the intermediate region. The remainder of this paper considers whether existing crystallographic information can be used to enhance the predictive power of the ΔpK_a rule in the intermediate region.

Ionisation and solvation statistics in the CSD (dataset-1)

Dataset-1 contains 258 719 crystal structures of organic compounds containing between one and four different molecular components. Dataset-1 was analysed by crystal type and composition, as described in the Methods section. Crystals with only one main component were classified either as neutral (no proton transfer) or zwitterionic, with the further distinction that some zwitterions are not the result of proton transfer (referred to as zwitterion-Q4). Multi-component systems were classified as co-crystals (neutral main components), co-crystals containing zwitterions, salts, salts-Q4 (quaternary salts) and ionic co-crystals. Some more
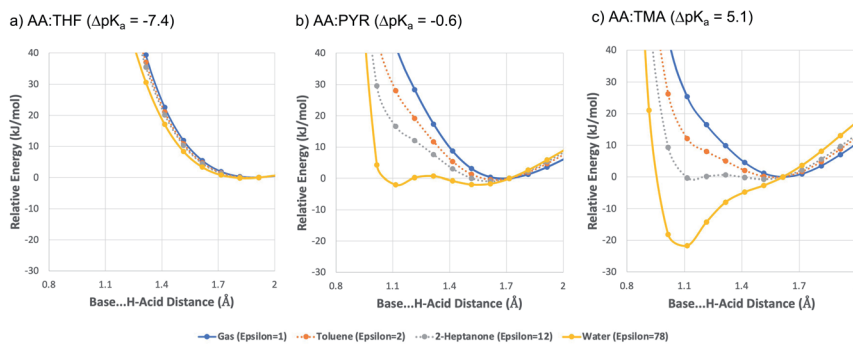

Fig. 5 Computed potential energy curves for the proton transfer reaction (as a function of the H⋯B distance) between the three acid–base pairs in four different solvation environments. The energy is given relative to the most stable neutral acid–base pair configuration. The implicit SMD solvation model is used at the #B97d/6-31+G(d,p) level of theory.

Table 1 Crystal types classified by their ionisation state and composition, number of crystal structures in dataset-1 (N) and percentage of those observed as unsolvated, hydrates or solvates

Crystal type	#MC[a]	Composition[b]	N	Percentage of dataset (%)		
				Unsolvated	Hydrate	Solvate
Neutral	1	N	215 491	92	4	5
Zwitterion	1	Z	2112	60	34	6
Zwitterion-Q4	1	Q4–Z	3677	86	10	4
Co-crystal	2	N N	9464	89	6	5
Co-crystal with Z	2	N Z	349	73	21	6
Co-crystal with ZQ4	2	N Q4–Z	197	85	7	8
Salt	2	$C^+ A^-$	16 610	72	23	5
Salt Q4	2	$Q4–C^+ A^-$	6479	65	27	8
Salt with Z	2	$Z^+ A^-$	181	66	33	1
Salt with Z	2	$C^+ Z^-$	138	69	28	3
Salt with Z	2	$Q4–Z^+ A^-$	123	64	33	3
Co-crystal	3	N N N	248	91	6	3
Ionic co-crystal	3	$C^+ A^-$ N	1364	76	20	4
Ionic co-crystal	3	$C^+ A^-$ Z	85	82	18	0
Ionic co-crystal	4	$C^+ A^-$ N N	46	100	0	0

[a] #MC = number of main components. [b] N = neutral non solvent or zwitterion; Z = zwitterion; Z^+ = cationic zwitterion; Z^- = anionic zwitterion; C^+ = cation; A^- = anion; Q4 = quaternary.

complex systems were found, for example salts with multiple anion/cations, but these were not analysed further. A summary of the classification data is given in Table 1.

The most common types of crystals in the dataset are those containing only one neutral component, followed by salts, co-crystals and quaternary salts. Of these crystal structures, 10% contain ionised species (salts or (zwitter)ionic co-crystals), of which almost 73% involve proton transfer and 27% are quaternary salts. The transfer of a single proton is most common amongst all of the salts, being observed in 74% of the structures, followed by the transfer of two protons in 23% of the structures. Zwitterions are observed in only 3% of the dataset, so structures with zwitterions remain relatively rare in the CSD. Zwitterionic compounds that are not a result of proton transfer (zwitterion-Q4) are more common than zwitterionic forms that arise from self-proton transfer. This is likely to be a simple consequence of the chemical space represented in the CSD, which reflects to a large extent the common preferences of synthetic chemists. Whilst quaternary systems are analysed here for the purpose of general statistics, these are not relevant to the ΔpK_a rule and thus are removed for the subsequent sections and analyses.

Most interesting in the current context is the relationship between salt/co-crystal formation and the hydration/solvation of the crystals. Whilst solvates make up only a small percentage of all crystal types, hydrates are much more common. In part, this is to be expected due the ubiquitous nature of water and its frequent use as a solvent, and several authors have discussed reasons why hydration is particularly common in molecular crystals.[21,56–59] However, while

hydrates constitute up to 6% of crystals containing only neutral (non-zwitterion) species, the percentage increases significantly to around 30% for crystals containing ions and/or zwitterions.

ΔpK_a in multi-component crystals

Dataset-2 is a subset of dataset-1 containing all structures with at least one acid–base pair, and thus one ΔpK_a value. This set was used to determine the relative occurrence of co-crystals, mono-ionised salts and multi-ionised salts as a function of ΔpK_a. The first comparison involves the relative distribution of co-crystals *versus* mono-ionised salts where ΔpK_a is calculated as the difference between the strongest acid and the strongest base (which must be in different molecules). The results are shown in Fig. 6, where the data have been separated into unsolvated (neat) co-crystals and salts (Fig. 6a) and hydrates of co-crystals and salts (Fig. 6b).

The result for neat co-crystals and salts is very similar to that presented by Cruz-Cabeza in 2012, with just a small shift to higher ΔpK_a values at which the percentage of the dataset is 50%:50% for co-crystals and salts. The percentage value in the plot can be considered as the probability for an acid/base system of a given ΔpK_a to be ionised when crystallised in an unsolvated form. In Fig. 6a, the co-crystal:salt equivalence point is observed at $\Delta pK_a \approx 1.4$, compared to $\Delta pK_a \approx 1$ in the 2012 study. Interestingly, the data for hydrates of co-crystals and salts is significantly shifted to the left, with the equivalence point in that distribution found at $\Delta pK_a \approx -0.5$. The intermediate region of the plot ($-3 < \Delta pK_a < 2$) deviates noticeably from a sigmoidal shape. This may be influenced by the relatively smaller sample size, or it may indicate a greater degree of uncertainty in the apparent trend when applied to crystalline hydrates.

ΔpK_a for second proton transfer ($\Delta pK_{a,\mathrm{II}}$)

For crystals in dataset-2 with the possibility for two proton transfers (*i.e.* with calculated values for both ΔpK_a and $\Delta pK_{a,\mathrm{II}}$), Fig. 7 shows the relative occurrence of mono-ionised salts *versus* di-ionised salts as a function of $\Delta pK_{a,\mathrm{II}}$. The intent
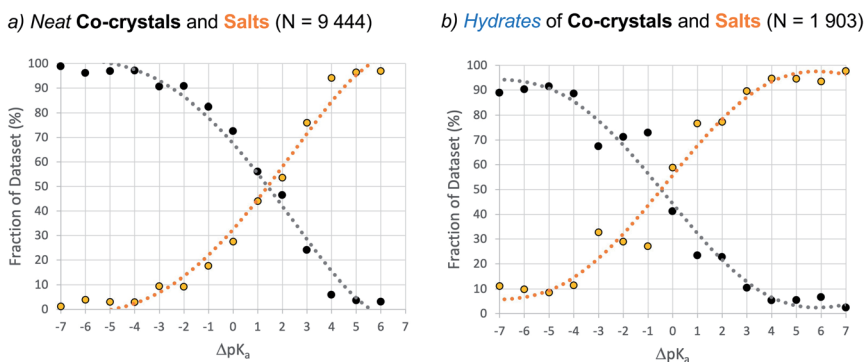

a) Neat **Co-crystals** and **Salts** (N = 9 444) b) *Hydrates* of **Co-crystals** and **Salts** (N = 1 903)

Fig. 6 Relative occurrence (%) of co-crystals (black) *versus* salts (orange) as a function of ΔpK_a (bins of one ΔpK_a unit) and hydration. Dataset-2 is filtered according to: no zwitterions, no Q4 ions, no other solvents, no or one proton transfer.

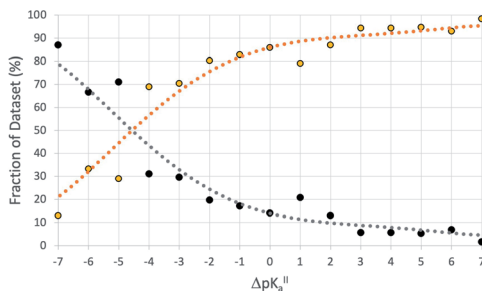**_Salts_ (single ionisation) and Salts (multiple ionisations) (N = 1 372)**

Fig. 7 Relative occurrence (%) of salts with a single ionisation (black) *versus* salts with multiple ionisations (orange) as a function of $\Delta pK_{a,II}$ (bins of one $\Delta pK_{a,II}$ unit). Dataset-2 is filtered according to: no zwitterions, no Q4 ions, no other solvents, one or more proton transfer.

here is to examine the effect of the crystal lattice of the mono-ionised salt on the second ionisation of an acid/base system. The number of observations in this case is reduced considerably compared to the co-crystal/salt dataset in Fig. 6, and thus more noise is seen on the apparent sigmoidal curves. Also, because of the smaller number of observations, the data are not separated into unsolvated *versus* hydrated forms. The data in Fig. 7 show a considerable shift to $\Delta pK_{a,II} = -4.5$ for the crossing point between the mono-ionised and di-ionised salts compared to that for the formation of any salt *versus* co-crystal as a function of ΔpK_a. Fig. 8 shows the number of proton transfers (0, 1 or 2) plotted against ΔpK_a and $\Delta pK_{a,II}$ in this dataset. Considering only ΔpK_a, the 50% probability of forming any salt (one or two proton transfers) falls between $\Delta pK_a = 0$ to 1, consistent with the expectations for co-crystals and salts seen in Fig. 6a. When looking at $\Delta pK_{a,II}$, however, the point of 50% probability for forming any salt (either one or two proton transfers) remains around $\Delta pK_{a,II} \approx 0$, but the probability of forming a salt with two proton transfers is clearly much greater than that of forming a salt with one proton transfer. Hence, where there is the possibility for two proton transfers, the choice is more frequently between a co-crystal and a divalent salt, with monovalent salts being far less common. This is consistent with the indications in Fig. 7, and highlights that the ΔpK_a rule does not apply within the same limits for ΔpK_a and $\Delta pK_{a,II}$ where there is a possibility for a second proton
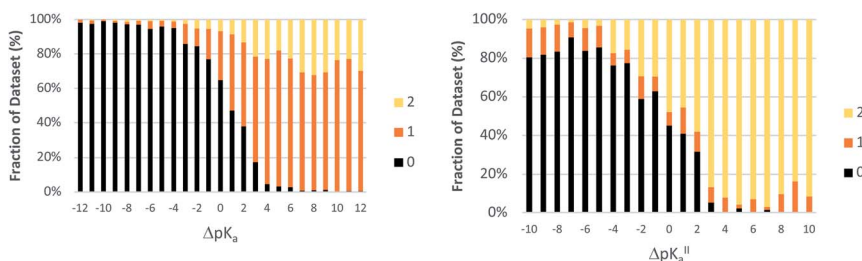

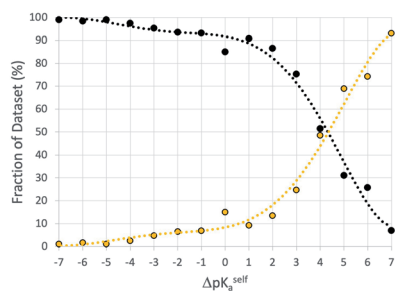
Fig. 8 Relative occurrence (%) of salts with 0, 1 or 2 proton transfers as a function of ΔpK_a and $\Delta pK_{a,II}$ (bins of one ΔpK_a value). The dataset is the same as that used to produce Fig. 7.

a) *Neat* **Non-zwitterions** and **Zwitterions** (N = 18 231)   b) *Hydrates* of **Non-Zwitterions** and **Zwitterions** (N = 2 359)

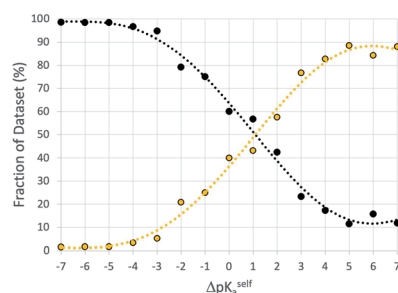**Fig. 9** Relative occurrence (%) of non-zwitterions (black) *versus* zwitterions (orange) as a function of $\Delta pK_{a,self}$ (bins of one ΔpK_a unit). Data for unsolvated forms (a) are compared to hydrates (b). Dataset-2 is filtered according to: only one main component, no Q4 zwitterions.

transfer. Here, of course, the stoichiometry of the acid : base could play a key role when the acid and/or base itself does not have two acid/basic sites but rather two molecules of the acid/base are required per molecule of base/acid. Practically, this emphasises the importance of exploring a larger range of acid–base ratios and stoichiometries during salt screening, especially for potential divalent salts.

ΔpK_a in zwitterions

Data were retrieved for unsolvated forms (one main component only) and hydrates (one main component plus water) of molecules potentially able to exist as a zwitterion (*i.e.* with a calculated $\Delta pK_{a,self}$ value). Fig. 9 shows that the equivalence point in the distribution of neutral and zwitterionic forms occurs at $\Delta pK_{a,self} \approx 4.1$, which is significantly higher than that found for multi-component crystals. Again, hydration has the same effect as in multi-component systems, lowering the equivalence point in the zwitterion set to $\Delta pK_{a,self} \approx 1$. It must be stressed that the data computed here are macro ionisation constants, which refer to the behaviour of the whole molecule to act as an acid or base, without any information on the microspecies that may be involved. Where the acid and base groups are sufficiently far apart within the molecule, it could be assumed that they would act independently, so $\Delta pK_{a,self}$ is a meaningful measure. Where the acid and base groups are not independent (*e.g.* in close proximity in the molecule or linked through resonance effects), this could have a significant influence on $\Delta pK_{a,self}$. Hence, while Fig. 9 serves as a guideline for potential self-proton transfer, the application of $\Delta pK_{a,self}$ to predict zwitterion formation should be viewed with a greater degree of caution since here the micro-ionisation constants play an important role.

Discussion

When transferring ΔpK_a values from the aqueous environment to make predictions about potential proton transfer in the solid state, the significant change in solvation environment can impact the overall expectations. Analysis of crystal structures in the CSD suggests in general that when ΔpK_a is sufficiently negative (<-1) or sufficiently positive ($>+4$), the influence of this change in environment is

unlikely to overturn the indication of salt/co-crystal formation provided by ΔpK_a. When ΔpK_a lies in the intermediate range, however, the thermodynamic preference for proton transfer is strongly dependent on the solvation environment. The important new result in this paper is the demonstration that crystal composition has an important influence on the ΔpK_a rule. Most notably, the point of 50% probability for salt formation is shifted to lower ΔpK_a for crystalline hydrates compared to unsolvated forms. Indeed, the data show that salt formation in crystalline hydrates mirrors almost perfectly aqueous solution data: thus, for crystalline hydrates of acid/bases, $\Delta pK_a > 0$ should result in a salt and $\Delta pK_a < 0$ should result in a co-crystal. This finding begs the question as to which is the consequence of which: does hydration occur because of proton transfer? Or does proton transfer occur because of hydration?

In the regions where the non-ionised versus the ionised probabilities cross, a linear correlation can be found. The fitted equations in Table 2 may prove valuable for prediction of proton transfer in molecular crystals of various nature and compositions.
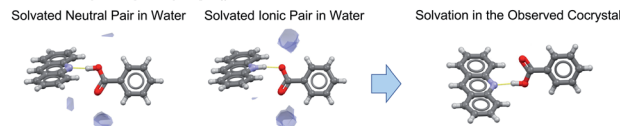
Concerning unsolvated co-crystals versus salts, the data suggest that unsolvated forms of acid–base pairs are usually worse at solvating the ionic species than water. To compensate for this, ΔpK_a must be positive for ionisation to occur.

Table 2 Linear fitting results for the intermediate ΔpK_a regions (ranges given) for the different ionisation systems. The fitted equations represent the probability of ionisation to occur at that given ΔpK_a. Above the intermediate ΔpK_a region, ionisation almost always occurs, whilst below the region, ionisation almost never occurs

System: neutral (a) vs. ionised (b)	Range	ΔpK_a cross	$P_{obs}{}^a$ (ion, %)	R^2
Monovalent vs. multivalent salt	$[-7, 0]$	-4.2	$11\Delta pK_a^{II} + 96$	0.89
Hydrated co-crystal vs. hydrated monovalent salt	$[-5, 4]$	-0.6	$10\Delta pK_a + 56$	0.94
Hydrated neutral vs. hydrated zwitterion	$[-3, 5]$	1.1	$11\Delta pK_a^{self} + 38$	0.98
Cocrystal vs. monovalent salt	$[-2, 4]$	1.3	$14\Delta pK_a + 32$	0.98
Neutral vs. zwitterion	$[1, 7]$	4.1	$15\Delta pK_a^{self} - 12$	0.97

^{a} Ionisation, second ionisation or self-ionisation as appropriate.

PUTMAU (Cocrystal): $\Delta pK_a = 2.0$
Solvated Neutral Pair in Water   Solvated Ionic Pair in Water   Solvation in the Observed Cocrystal

HONWEN (Salt): $\Delta pK_a = 1.1$
Solvated Neutral Pair in Water   Solvated Ionic Pair in Water   Solvation in the Observed Salt

Fig. 10 Visualisation of water solvation of non-ionised versus ionised acid–base pairs with full interaction maps versus the resulting ionisation and interactions observed in their crystals.

Table 3 Salts and co-crystals with $-0.5 < \Delta pK_a < 0.5$ where the acid is an organic carboxylic acid. Statistics relate to the % of those carboxylic acids involved in 3, 2, 1 or 0 ancillary hydrogen bonds (aHBs)

	N total	Salt%	Co-crystal%
2 aHBs A/A$^-$	147	54%	46%
1 aHBs A/A$^-$	247	12%	88%
0 aHBs A/A$^-$	137	3%	96%

In order to illustrate this observation, we have selected two examples of benzoic acid forming a salt and a co-crystal with two different bases with ΔpK_a values between 1 and 2. Using the Mercury full interaction maps (FIMs) tool with a water oxygen as probe, we can visualise the ancillary hydrogen bonds (aHBs) where water is involved with the acid–base pair in aqueous solution in its non-ionised form *versus* its ionised form (Fig. 10). In aqueous solution, water forms one aHB with the carbonyl of the carboxylic acid in its neutral form whilst forming two strong aHBs with the carboxylate. For the crystal outcome to be predicted solely by ΔpK_a, the level of solvation of the acid–base pair in solution must be maintained in the solid state. In such a scenario, a positive ΔpK_a will imply salt formation, whilst a negative ΔpK_a will imply co-crystal formation. If solvation in the crystal is worse than in water (fewer aHBs), then the ΔpK_a value for the switch between salt and co-crystal must be shifted to higher values. In PUTMAU (Fig. 10), for example, there are no other HB donors in the acid or base, so no aHBs are possible and, thus, the outcome is a co-crystal. In HOMWEN (Fig. 10), however, there is a hydroxyl group available on the base able to form an aHB with the carboxylate, and thus a salt is observed in the solid state. For an acid and base with a ΔpK_a between 1 and 2, the experimentally derived probability for a salt to form would be between 50–60% (Table 2). In that scenario, a higher number of aHBs should result in a salt, whilst a lower number should result in a co-crystal.

To illustrate further the importance of crystalline aHBs to the ionisation outcome, we analyse the number of aHBs in acid–base co-crystals and salts with a $\Delta pK_a \approx 0$ (Table 3). 147 crystal structures were found where the carboxylic acid/carboxylate was involved in two aHBs, 247 in one aHB and 137 in no aHBs (Table 3).

Acid–base crystalline complexes able to afford two aHBs generate a solvation environment similar to water. Interestingly, nearly 50% of the 147 crystals with two aHBs are salts and the other 50% are co-crystals, mirroring the behaviour expected in aqueous solution where $\Delta pK_a \approx 0$. When only one or no aHBs are possible, co-crystals clearly dominate over salts. Here, when a reduction of aHBs occurs, the nature and strength of those aHBs would matter, with stronger HBs better able than weaker aHBs to stabilise the ionic species. This effect is clearly seen in the case of double ionisation where the $\Delta pK_{a,II}$ values for the switch between salt and co-crystal are shifted to negative values.

Conclusions

The ΔpK_a rule is widely used in crystal engineering for the design of salts and co-crystals, particularly for pharmaceutical compounds. Its origin is experimental, but associated with the thermodynamics of acid–base aqueous equilibria. There is indeed a simple thermodynamic relationship between ΔpK_a for an acid and a base

and the corresponding free energy for proton transfer in aqueous solution ($\Delta G^{\circ \, HA \cdot B}_{ion\text{-}water} = -2.3RT\Delta pK_a$). Transferring this relationship to the solid state, although clearly convenient, comes with several challenges. Solvation plays a key role in the ionisation reaction and moving the acid–base species from aqueous solution (where the ΔpK_a defines their relative acid strength) into the crystals shifts the ΔpK_a expectations for ionisation to occur (as seen from experimentation). This experimental shift observation is what we refer to as the ΔpK_a rule. The rule works well for more extreme cases of ΔpK_a but loses its predictive power at ΔpK_a values between -1 and 4, where proton transfer in the solid state becomes a fine balance between the "inherent" tendency for proton transfer and the influence of the crystalline environment.

To illustrate the important role of the solvation environment on the ionisation outcome in the crystalline state, we have examined the applicability of the ΔpK_a rule in crystalline systems with different compositions. This reveals that the point of equal probability of salt/co-crystal formation lies at $\Delta pK_a \approx 1.1$ for neat (unsolvated) forms, but at around 0 for hydrates. In zwitterions, an even more positive ΔpK_a value of 4.1 is seen, whilst in multi-protic salts the point is negative, around $\Delta pK_a \approx -4.2$. New probability equations for ionisation (based on linear fittings to the CSD observations) are provided to enhance the predictive power of the ΔpK_a rule in the intermediate region for systems of various compositions.

We have also highlighted the importance of solvation in this intermediate region of ΔpK_a values for a few illustrative examples. Acid–base pairs that are stabilised by strong solvation in the crystalline state are more likely to be ionised than acid–base pairs that are not involved in any ancillary hydrogen bonds in the crystal. Finally stoichiometry and its impact to the hydrogen-bonding environment of the acid–base complex can also play a role.[60] We anticipate that this contribution will be useful for future applications of the ΔpK_a rule. The herein derived probability equations for crystals of various compositions, combined with an analysis of possible aHBs, can undoubtedly enhance the ΔpK_a rule's predictive power in the intermediate region.

Author contributions

AJCC initiated the project and performed the CSD searches and calculations. All authors contributed to the discussions, drafting of the paper and improvement of the data and made important contributions to the theoretical fundamentals. The authors thank Prof. Roger Davey for helpful discussions.

Conflicts of interest

There are no conflicts to declare.

Acknowledgements

Notes and references

1 J. Manchester, G. Walkup, O. Rivin and Z. You, *J. Chem. Inf. Model.*, 2010, **50**, 565–571.

2   D. D. Perrin, B. Dempsey and E. P. Serjeant, *pK_a Prediction for Organic Acids and Bases*, Springer, 1981, vol. 1.

3   C. Lim, D. Bashford and M. Karplus, *J. Phys. Chem.*, 1991, **95**, 5610–5620.

4   D. A. Haynes, W. Jones and W. D. S. Motherwell, *J. Pharm. Sci.*, 2005, **94**, 2111–2120.

5   C. R. Groom, I. J. Bruno, M. P. Lightfoot and S. C. Ward, *Acta Crystallogr., Sect. B: Struct. Sci., Cryst. Eng. Mater.*, 2016, **72**, 171–179.

6   M. Sadakiyo, T. Yamada and H. Kitagawa, *J. Am. Chem. Soc.*, 2009, **131**, 9906–9907.

7   J. S. Stevens, S. Coultas, C. Jaye, D. A. Fischer and S. L. M. Schroeder, *Phys. Chem. Chem. Phys.*, 2020, **22**, 4916–4923.

8   J. S. Stevens, M. Walczak, C. Jaye and D. A. Fischer, *Chem.–Eur. J.*, 2016, **22**, 15600–15604.

9   C. C. Wilson, N. Shankland and A. J. Florence, *J. Chem. Soc., Faraday Trans.*, 1996, **92**, 5051–5057.

10 J. S. Stevens, S. J. Byard and S. L. M. Schroeder, *J. Pharm. Sci.*, 2010, **99**, 4453–4457.

11 S. Tothadi, T. R. Shaikh, S. Gupta, R. Dandela, C. P. Vinod and A. K. Nangia, *Cryst. Growth Des.*, 2021, **21**, 735–747.

12 P. T. Edwards, L. K. Saunders, A. R. Pallipurath, A. J. Britton, E. A. Willneff, E. J. Shotton and S. L. M. Schroeder, *Cryst. Growth Des.*, 2021, **21**(11), 6332–6340.

13 L. Rajput, M. Banik, J. R. Yarava, S. Joseph, M. K. Pandey, Y. Nishiyama and G. R. Desiraju, *IUCrJ*, 2017, **4**, 466–475.

14 L. H. Thomas, A. J. Florence and C. C. Wilson, *New J. Chem.*, 2009, **33**, 2486–2490.

15 M.-M. Blum, M. Mustyakimov, H. Rüterjans, K. Kehe, B. P. Schoenborn, P. Langan and J. C.-H. Chen, *Proc. Natl. Acad. Sci. U. S. A.*, 2009, **106**, 713–718.

16 S. M. Reutzel-Edens, *Pharmaceutical Salts and Co-crystals*, Royal Society of Chemistry, 2011, pp. 212–246.

17 T. Wang, J. S. Stevens, T. Vetter, G. F. S. Whitehead, I. J. Vitorica-Yrezabal, H. Hao and A. J. Cruz-Cabeza, *Cryst. Growth Des.*, 2018, **18**, 6973–6983.

18 S. M. Berge, L. D. Bighley and D. C. Monkhouse, *J. Pharm. Sci.*, 1977, **66**, 1–19.

19 A. T. Serajuddin, *Adv. Drug Delivery Rev.*, 2007, **59**, 603–616.

20 D. P. Elder, R. Holm and H. L. De Diego, *Int. J. Pharm.*, 2013, **453**, 88–100.

21 C. B. Aakeröy, M. E. Fasulo and J. Desper, *Mol. Pharmaceutics*, 2007, **4**, 317–322.

22 G. R. Desiraju, *Angew. Chem., Int. Ed.*, 2007, **46**, 8342–8356.

23 G. R. Desiraju, *J. Am. Chem. Soc.*, 2013, **135**, 9952–9967.

24 M. Karimi-Jafari, L. Padrela, G. M. Walker and D. M. Croker, *Cryst. Growth Des.*, 2018, **18**, 6370–6387.

25 M. K. Corpinot and D.-K. Bučar, *Cryst. Growth Des.*, 2019, **19**, 1426–1453.

26 A. Nangia and G. R. Desiraju, Supramolecular Synthons and Pattern Recognition, in *Topics in Current Chemistry*, E. Weber, Springer, Berlin, 1999, vol. 198.

27 G. R. Desiraju, *Angew. Chem., Int. Ed. Engl.*, 1995, **34**, 2311–2327.

28 J. A. Bis, P. Vishweshwar, D. Weyna and M. J. Zaworotko, *Mol. Pharmaceutics*, 2007, **4**, 401–416.

29 P. Gilli, L. Pretto and G. Gilli, *J. Mol. Struct.*, 2007, **844–845**, 328–339.

30 P. Gilli, L. Pretto, V. Bertolasi and G. Gilli, *Acc. Chem. Res.*, 2009, **42**, 33–44.

31 B. R. Bhogala, S. Basavoju and A. Nangia, *CrystEngComm*, 2005, **7**, 551–562.

32 A. J. Cruz-Cabeza, *CrystEngComm*, 2012, **14**, 6362–6365.

33 S. L. Childs, G. P. Stahly and A. Park, *Mol. Pharmaceutics*, 2007, **4**, 323–338.

34 G. Ramon, K. Davies and L. R. Nassimbeni, *CrystEngComm*, 2014, **16**, 5802–5810.

35 A. Lemmerer, S. Govindraju, M. Johnston, X. Motloung and K. L. Savig, *CrystEngComm*, 2015, **17**, 3591–3595.

36 A. Mukherjee and G. R. Desiraju, *Cryst. Growth Des.*, 2014, **14**, 1375–1385.

37 *ChemAxon version 21.13*, https://www.chemaxon.com.

38 M. J. Frisch, G. W. Trucks, H. B. Schlegel, G. E. Scuseria, M. A. Robb, J. R. Cheeseman, G. Scalmani, V. Barone, G. A. Petersson, H. Nakatsuji, X. Li, M. Caricato, A. V. Marenich, J. Bloino, B. G. Janesko, R. Gomperts, B. Mennucci, H. P. Hratchian, J. V. Ortiz, A. F. Izmaylov, J. L. Sonnenberg, D. Williams-Young, F. Ding, F. Lipparini, F. Egidi, J. Goings, B. Peng, A. Petrone, T. Henderson, D. Ranasinghe, V. G. Zakrzewski, J. Gao, N. Rega, G. Zheng, W. Liang, M. Hada, M. Ehara, K. Toyota, R. Fukuda, J. Hasegawa, M. Ishida, T. Nakajima, Y. Honda, O. Kitao, H. Nakai, T. Vreven, K. Throssell, J. A. Montgomery, Jr, J. E. Peralta, F. Ogliaro, M. J. Bearpark, J. J. Heyd, E. N. Brothers, K. N. Kudin, V. N. Staroverov, T. A. Keith, R. Kobayashi, J. Normand, K. Raghavachari, A. P. Rendell, J. C. Burant, S. S. Iyengar, J. Tomasi, M. Cossi, J. M. Millam, M. Klene, C. Adamo, R. Cammi, J. W. Ochterski, R. L. Martin, K. Morokuma, O. Farkas, J. B. Foresman, and D. J. Fox, *Gaussian 16*, Revision C.01, Gaussian, Inc., Wallingford CT, 2016.

39 S. Grimme, *J. Comput. Chem.*, 2006, **27**, 1787–1799.

40 A. V. Marenich, C. J. Cramer and D. G. Truhlar, *J. Phys. Chem. B*, 2009, **113**, 6378–6396.

41 *Avogadro version 1.1.1*, https://avogadro.cc.

42 M. D. Hanwell, D. E. Curtis, D. C. Lonie, T. Vandermeersch, E. Zurek and G. R. Hutchison, *J. Cheminf.*, 2012, **4**, 17.

43 T. A. Halgren, *J. Comput. Chem.*, 1996, **17**, 490–519.

44 C. R. Groom, I. J. Bruno, M. P. Lightfoot and S. C. Ward, *Acta Crystallogr., Sect. B: Struct. Sci., Cryst. Eng. Mater.*, 2016, **72**(2), 171–179.

45 P. A. Wood, T. S. G. Olsson, J. C. Cole, S. J. Cottrell, N. Feeder, P. T. A. Galek, C. R. Groom and E. Pidcock, *CrystEngComm*, 2013, **15**, 65–72.

46 C. F. Macrae, I. Sovago, S. J. Cottrell, P. T. A. Galek, P. McCabe, E. Pidcock, M. Platings, G. P. Shields, J. S. Stevens, M. Towler and P. A. Wood, *J. Appl. Crystallogr.*, 2020, **53**, 226–235.

47 B. G. Cox, *Acids and Bases: Solvent Effects on Acid-Base Strength*, Oxford University Press, Oxford, New York, 2013.

48 Y. Abramov, G. Sun, Y. Zhou, M. Yang, Q. Zeng and Z. Shen, *Cryst. Growth Des.*, 2019, **19**, 7132–7137.

49 I. E. Charif, S. M. Mekelleche, D. Villemin and N. Mora-Diez, *J. Mol. Struct.: THEOCHEM*, 2007, **818**, 1–6.

50 S. Mohamed, D. A. Tocher, M. Vickers, P. G. Karamertzanis and S. L. Price, *Cryst. Growth Des.*, 2009, **9**, 2881–2889.

51 L. Mazur, I. Materek, A. D. Bond and W. Jones, *Cryst. Growth Des.*, 2019, **19**, 2663–2678.

52 A. M. Reilly, R. I. Cooper, C. S. Adjiman, S. Bhattacharya, A. D. Boese, J. G. Brandenburg, P. J. Bygrave, R. Bylsma, J. E. Campbell, R. Car, D. H. Case, R. Chadha, J. C. Cole, K. Cosburn, H. M. Cuppen, F. Curtis, G. M. Day, R. A. DiStasio Jr, A. Dzyabchenko, B. P. van Eijck, D. M. Elking, J. A. van den Ende, J. C. Facelli, M. B. Ferraro, L. Fusti-Molnar, C.-A. Gatsiou, T. S. Gee, R. de Gelder, L. M. Ghiringhelli, H. Goto, S. Grimme, R. Guo, D. W. M. Hofmann, J. Hoja, R. K. Hylton, L. Iuzzolino, W. Jankiewicz, D. T. de Jong, J. Kendrick, N. J. J. de Klerk, H.-Y. Ko, L. N. Kuleshova, X. Li, S. Lohani, F. J. J. Leusen, A. M. Lund, J. Lv, Y. Ma, N. Marom, A. E. Masunov, P. McCabe, D. P. McMahon, H. Meekes, M. P. Metz, A. J. Misquitta, S. Mohamed, B. Monserrat, R. J. Needs, M. A. Neumann, J. Nyman, S. Obata, H. Oberhofer, A. R. Oganov, A. M. Orendt, G. I. Pagola, C. C. Pantelides, C. J. Pickard, R. Podeszwa, L. S. Price, S. L. Price, A. Pulido, M. G. Read, K. Reuter, E. Schneider, C. Schober, G. P. Shields, P. Singh, I. J. Sugden, K. Szalewicz, C. R. Taylor, A. Tkatchenko, M. E. Tuckerman, F. Vacarro, M. Vasileiadis, A. Vazquez-Mayagoitia, L. Vogt, Y. Wang, R. E. Watson, G. A. de Wijs, J. Yang, Q. Zhu and C. R. Groom, *Acta Crystallogr., Sect. B: Struct. Sci., Cryst. Eng. Mater.*, 2016, **72**, 439–459.

53 L. M. LeBlanc, S. G. Dale, C. R. Taylor, A. D. Becke, G. M. Day and E. R. Johnson, *Angew. Chem., Int. Ed.*, 2018, **57**, 14906–14910.

54 P. Praphanwittaya, P. Saokham, P. Jansook and T. Loftsson, *J. Drug Delivery Sci. Technol.*, 2021, **62**, 102359.

55 T. G. Cooper, K. E. Hejczyk, W. Jones and G. M. Day, *J. Chem. Theory Comput.*, 2008, **4**, 1795–1805.

56 G. R. Desiraju, *J. Chem. Soc., Chem. Commun.*, 1991, 426–428.

57 L. Infantes, L. Fábián and W. D. Sam Motherwell, *CrystEngComm*, 2007, **9**, 65–71.

58 A. Bajpai, H. S. Scott, T. Pham, K.-J. Chen, B. Space, M. Lusi, M. L. Perry and M. J. Zaworotko, *IUCrJ*, 2016, **3**, 430–439.

59 H. D. Clarke, K. K. Arora, H. Bass, P. Kavuru, T. T. Ong, T. Pujari, L. Wojtas and M. J. Zaworotko, *Cryst. Growth Des.*, 2010, **10**, 2152–2167.

60 P. Stainton, E. Nauha, T. Grecu, J. F. McCabe, T. Munshi, I. Scowen, H. C. Stephen Chan, S. Nilsson and N. Blagden, *Cryst. Growth Des.*, 2022, **22**(3), 1665–1679.